Effects of Cu^{2+} Ions on the Structure and Reactivity of Todorokite- and Cryptomelane-Type Manganese Oxide Octahedral Molecular Sieves

Elaine Nicolas-Tolentino, Zheng-Rong Tian, Hua Zhou, Guanguang Xia, and Steven L. Suib*

U-60, Department of Chemistry, University of Connecticut, Storrs, Connecticut 06269-3060

Received December 2, 1998. Revised Manuscript Received April 22, 1999

The concentration effects on Cu uptake into the structures and reactivity of manganese oxide octahedral molecular sieves (OMS) were investigated. Two sets of 3 × 3-tunnel structure OMS designated as OMS-1 were synthesized by hydrothermal treatment at 160 °C for 48 h. The Cu−OMS-1 series of materials (tunnel substituted) were prepared by incorporating Cu^{2+} ions into OL-1, which has a layered structure, at 60 °C for 24 h. [Cu]−OMS-1 materials (framework substituted) were prepared by ion exchanging Cu^{2+} ions into the tunnels of OMS-1 under similar conditions. Cu−OMS-2 materials characterized by 2 × 2 tunnels were prepared by the reflux method. ICP analysis shows a Cu/Mn molar ratio of 0.278 for Cu−OMS-1 labeled **C** as the substitution limit for a pure sample based on its XRD pattern. The Cu(II) ions easily substitute for the divalent cations (Mg^{2+}, Mn^{2+}) either in tunnel or framework sites when exchange was done before hydrothermal treatment. The presence of Cu^{2+} ions decreases the Mn^{2+}/Mn^{4+} ratio in Cu−OMS-1 samples as suggested by an increasing trend in the average oxidation state of Mn and decreasing amounts of total Mn. XPS data reveal that Cu remains in the 2^+ state in all of the materials as indicated by the shake-up peaks associated with Cu in such valency. EPR spectra of Cu-containing OMS-1 materials show the six peaks of Mn^{2+} with a hyperfine splitting constant of 97 G, indicating an octahedral environment. The TGA profiles of [Cu]−OMS-1 show that these samples have the same thermal stability as OMS-1 but the amount of lattice oxygen evolved decreases slightly with the amount of Cu^{2+} in the tunnel. The thermal stability of the Cu− OMS-1 and Cu−OMS-2 structures decrease as the amount of Cu incorporated increases. The copper ions that substitute for Mn^{2+} in the framework are considered as defects in the structure of the crystallites which make them less stable than OMS-1 containing Mg^{2+} in the framework where it exhibits a stabilizing effect. Resistivity measurements show a decrease and leveling off as the concentration of Cu increases in the Cu−OMS-1 series, which is a trend consistent with doping. The resistivity of the OMS-2 structure increases with the amount of copper incorporated. Cu(II) ions replacing the divalent cations in the framework during hydrothermal synthesis possibly account for the properties observed in the Cu−OMS-1 materials. An increased catalytic activity was observed for this set of materials as the Cu/Mn ratio increased for the oxidative dehydrogenation of ethylbenzene to styrene at 300 °C at 1 atm.

Introduction

A series of manganese octahedral molecular sieves (OMS)[1−9] have been synthesized with MnO_6 octahedra sharing corners and edges to form tunnel structures of varying sizes. Synthetic todorokite, which has a 3 × 3 tunnel structure having a pore size of about 6.9 Å, is designated as OMS-1. Synthetic cryptomelane which is a related 2 × 2 structure of the mineral hollandite in the K^+ form, having a tunnel pore size of about 4.6 Å, is referred to as OMS-2.

Natural todorokite found in deep-sea nodules has been found to contain Ni, Co, Cu, Zn, Al, and Mg.[10−12] The cation content varied considerably in these samples. Some of these cations have been found to be mobile and

* To whom correspondence should be addressed.

(1) Shen, Y. F.; Zerger, R. P.; Suib, S. L.; McCurdy, L.; Potter, D. I.; O'Young, C. L. *J. Chem. Soc., Chem. Commun.* **1992**, 1213−1214.
(2) Shen, Y. F.; Zerger, R. P.; Suib, S. L.; McCurdy, L.; Potter, D. I.; O'Young, C. L. *Science* **1993**, *260*, 511−515.
(3) De Guzman, R.; Shen, Y. F.; Suib, S. L.; Shaw, B. R.; O'Young, C. L. *Chem. Mater.* **1993**, *5*, 1395−1400.
(4) Yin, Y. G.; Xu, W. Q.; De Guzman, R. N.; Suib, S. L.; O'Young, C. L. *Zeolites and Microporous Materials: State of the Art 1994*; Weitkamp, J., Ed.; Studies in Surface Science and Catalysis; Elsevier: Amsterdam, 1994; Vol. 84, pp 453−460.
(5) De Guzman, R. N.; Shen, Y. F.; Neth, E. J.; Suib, S. L.; O'Young, C. L.; Levine, S.; Newsam, J. M. *Chem. Mater.* **1994**, *6*, 815−821.
(6) Yin, Y. G.; Xu, W. Q.; De Guzman, R. N.; Suib, S. L.; O'Young, C. L. *Inorg. Chem.* **1994**, *33*, 4384−4389.
(7) De Guzman, R. N.; Awaluddin, A.; Shen, Y. F.; Tian, Z. R.; Suib, S. L.; Ching, S.; O'Young, C. L. *Chem. Mater.* **1995**, *7*, 1286−1292.
(8) Shen, Y. F.; De Guzman, R. N.; Zerger, R. P.; Suib, S. L.; O'Young, C. L. *Zeolites Microporous Cryst.* **1994**, 19−24.
(9) Shen, Y. F.; Suib, S. L.; O'Young, C. L. *J. Am. Chem. Soc.* **1994**, *116*, 11020−11029.
(10) Chikhrov, F. V.; Gorshkov, A. I.; Sivtsov, A. V.; Berenevskaya, V. V. *Nature* **1974**, *278*, 631−632.
(11) Post, J. E.; Bish, D. L. *Am. Mineralog.* **1988**, *73*, 861−869.
(12) Skinner, H. C. W., Fitzpatrick, R. W., Eds. *Biomineralization Processes of Iron and Manganese Catena*; Verlag: Germany, 1992.

10.1021/cm9811040 CCC: $18.00
Published on Web 06/09/1999

stabilize the structure of the nodule and layered materials.[2,3,12] Such cations may even be incorporated into the framework of todorokite by occupying the larger M2 and M4 sites[11] or probably by isomorphously substituting the Mn^{2+} cations found in the framework of todorokite.[1] One basis for such accommodation of inorganic cations is the relative size of the cations of Mg^{2+},Co^{2+}, Ni^{2+}, Cu^{2+}, and Zn^{2+} coordinated with six water molecules which are similar to the tunnel size of todorokite. In view of this, ion-exchanged OMS-1 materials having divalent ions substituting for Mn^{2+} have been prepared.

Shen et al.[9] have successfully used five hydrated inorganic divalent cations, Mg^{2+},Co^{2+}, Ni^{2+}, Cu^{2+}, and Zn^{2+}, as templates for the synthesis of OMS-1. Among the different tunnel cations, $Cu^{2+}$was reported in a different study to possess more available oxygen species that are reactive to H_2 and CO at low temperature.[13] OMS-1 prepared using hydrated Cu^{2+} as a template ion designated as Cu−OMS-1 catalyzes CO oxidation at 393 K in the presence of air.[2] The terminology M−OMS represents tunnel substitution, whereas [M]−OMS represents framework substitution. Cu−OMS-1 was further studied as a CO oxidation catalyst and showed a conversion of 89−99% at 60−100 °C.[14] Cu−OMS-2 was also reported to have the largest amount of oxygen available at low temperature and retains the tunnel structure up to 573 K compared to Ni−, K−,and Fe−OMS-2.[6] The OMS materials containing Cu clearly show interesting chemistry and applications. Hence, it is worth exploring concentration effects on the Cu uptake into the structures of these OMS materials. Substitution limits and effects on the structure, purity, thermal stability, and conductivity of Cu-containing OMS were investigated. Extensive characterization was carried out to differentiate the materials containing tunnel and framework Cu. The various Cu-containing OMS materials were evaluated as catalysts for the oxidative dehydrogenation of ethylbenzene to styrene at 300 °C and 1 atm. A detailed study of the mechanism and optimization of reaction conditions using the most active materials is reported.

II. Experimental Section

A. Preparation of Na−Birnessite (Na−OL-1). A layered manganese oxide material was first synthesized. A 200-mL solution A was prepared by dissolving 20 mmol of $KMnO_4$ in a NaOH solution with a final concentration of 4 M. Solution B contained 57 mmol of $MnCl_2 \cdot 4H_2O$ and 20 mmol of $MgSO_4 \cdot 7H_2O$ in 300 mL of distilled deionized water (DDW). Mg^{2+} is added to enhance thermal stability of the resultant oxide.[1−2] Solution B was added dropwise into solution A for 10 min under vigorous stirring. The mixture was allowed to stir for 1 h. The black-brown suspension was aged at room temperature for 4 days. The aged suspension was filtered and washed with DDW until the pH was about 7. A layered material, Na−birnessite, was then obtained which is an octahedral layered (OL) material and referred to as Na−OL-1.[1,2,3,5,7]

B. Preparation of Cu−OL-1 and Cu−OMS-1. Na−OL-1 suspension was ion-exchanged with 200 mL of $CuSO_4 \cdot 5H_2O$ solution with concentration ranging from 0.005 to 1.0 M at 60 °C while stirring overnight. The ion-exchanged product was filtered and washed with DDW at least 5 times. In this way, another layered material was obtained with Cu^{2+} in the interlayer. Evidence of Cu^{2+} in the interlayer comes from EPR, bulk analysis, electrochemical, transmission, electron microscopy, and other data.[3,5,7] Cu−OL-1 was autoclaved at 160 °C under autogenous pressure for 48 h to convert it to todorokite, which is a tunnel manganese oxide. The todorokite suspension was also filtered and washed with DDW three times and dried at ambient temperature in air.

C. Preparation of [Cu]−OL-1 and [Cu]−OMS-1. In the synthesis of [Cu]−OMS-1, OL-1 was ion-exchanged with $CuSO_4 \cdot 5H_2O$. The resulting [Cu]−Mg−OL-1 was autoclaved at 160 °C for 48 h, filtered, and washed with DDW. The resulting [Cu]−OMS-1 was produced as a black powder.

D. Preparation of Cu−OMS-2. Cu−OMS-2 was prepared by two methods. The first method involved a sol−gel synthesis of $KMNO_4$ and maleic acid.[15] The second method involved a reflux method using $KMnO_4$ and Mn^{2+} solutions.[5] To prepare the Cu^{2+}-substituted OMS-2 ([Cu]−OMS-2) materials, solutions of $CuSO_4 \cdot 5H_2O$ or $Cu(NO_3)_2$ were added to the initial solutions (either maleic acid or the Mn^{2+} solution) with final concentrations in solution ranging from 0.10 to 1.0 M. Resultant products were filtered, washed, and dried.

E. X-ray Diffraction (XRD) Studies. Samples were prepared by spreading a suspension of thoroughly ground powder on a glass slide to make a film and dried at room temperature. Powder X-ray diffraction data were collected using a Scintag XDS-2000 diffractometer with a Cu Kα radiation source operated at 45 kV, 40 mA, incident slits of 2 and 4 mm and a step size of 0.030°.

F. Inductively Coupled Plasma−Atomic Emission Spectroscopy (ICP-AES) Analysis. Powder samples were accurately weighed and dissolved in 5% HCl solution. A Perkin-Elmer 7-40 instrument equipped with an autosampler was used. Calibration checks using a known standard after every 10 runs and a blank check after every 5 runs were carried out.

G. Redox Titrations. The average oxidation state (AOS) of manganese was determined by a potentiometric titration employing a standard procedure for analysis of manganese in battery materials.[16] A detailed procedure has been described elsewhere.[2−3,5,7,9]

H. Thermal Analyses. Thermogravimetric analyses (TGA) and differential scanning calorimetry (DSC) were carried out with a High TGA 2950 Thermalgravimetric Analyzer and a DSC 2920 differential scanning calorimeter, respectively. About 20 mg of sample powder was loaded into a platinum sample holder for TGA. The TGA analyses were carried out in N_2 and O_2 atmosphere to monitor oxygen loss in the sample during heating. DSC was carried out only in N_2 with about 5 mg of the sample powder sealed in copper pans. Heating rates were 10 °C/min.

I. Scanning Electron Microscopy (SEM). The sample powders were spread uniformly on carbon paste in an aluminum sample holder. The mounted samples were gold coated to a thickness of about 1 nm. SEM micrographs were taken in an Amray 1645 Scanning Electron Microscope.

J. Resistivity Measurements. Samples weighing about 0.3 g were pressed into 1-mm-thick disks with 13 mm diameters using an applied force of 15000 psi for 2 min. The four-probe resistivity measurement was carried out using Keithley 136A multimeters. The circuit diagram for four-probe measurement has been given in the literature.[7]

K. Electron Paramagnetic Resonance (EPR) Measurements. Samples were vacuum-sealed in a quartz tube and diluted with silica in a 1:10 weight ratio. EPR spectra were obtained using a Bruker ESP 300 instrument equipped with an ER 023M signal channel, an ESP 10 MHz digitizer, an ER 032M field controller, and an ER 041 MR bridge. A temperature of 110 ± 0.5 K was achieved by employing a Eurotherm

(13) Yin, Y. G.; Xu, W. Q.; Shen, Y. F.; Suib, S. L.; O'Young, C. L. *Chem. Mater.* **1994**, *6*, 1803−1808.
(14) Shen, Y. F.; Suib, S. L.; O'Young, C. L. *J. Catal.* **1996**, *161*, 115−122.
(15) Duan, N. G.; Suib, S. L.; O'Young, C. L. *J. Chem. Soc. Chem. Commun.* **1995**, *13*, 1367−1368.
(16) Glover, D., Schumm, B., Jr., Kozowa, A., Eds. *Handbook of Manganese Dioxides Battery Grade*; International Battery Materials Association, 1989.

B-VT2000 nitrogen temperature controller. The following instrumental parameters were used: field modulation frequency of 100 kHz, gain set at 1.00×10^4, sweep time of 42 ms, and a time constant of 10 ms. Spectra were compiled as averages of 10 scans.

L. X-ray Photoelectron Spectroscopy (XPS). Samples were pressed in indium foil to minimize charging. XPS data were collected on a Leybold Heraeus (LH) Model 3000 spectrometer equipped with an LH EA-10 hemispherical analyzer. Narrow and wide scans of all elements were collected for the prominent photoelectron transitions and X-ray excited Auger transitions.

M. Oxidative Dehydrogenation of Ethylbenzene to Styrene. About 40.0 mg of the catalyst (300−590 μm) was loaded into a quartz reactor. A stream of ethylbenzene/O_2 gas mixture in He was flowed at a rate of 960 mL/h through the tubular reactor placed in a furnace at 300 °C. A GC equipped with a TCD was used to analyze the products. A more detailed description of the experiment has been described elsewhere.[17]

Results

A. Synthesis and Powder X-ray Diffraction. The syntheses of Cu−OMS-1 and [Cu]−OMS-1 materials are dependent on pH, rate of mixing, aging time and temperature, and source of substituting cations.[3,5,7] The Cu−OMS-1 materials were prepared at pH values of 3.0 and 4.0.[3] The samples synthesized at pH 4.0 were more crystalline and relatively purer than those prepared at a lower basicity on the basis of XRD results. The materials prepared at pH 3.0 were not completely converted to the tunnel phase as indicated by birnessite peaks at 6.9 (0 0 2) and 3.5 Å (2 1 2). Synthetic birnessite or OL-1, which is a precursor to the formation of the tunneled materials,[1,2] can be aged at room temperature for 4 days or at 60 °C for 2 days.[3,5,7] The rate of mixing the solutions also affects the quality of OL-1 produced.

If the $MnCl_2$ solution is added at a rapid rate, the formation of a very black precipitate occurs and after aging, several impurity peaks appear with the birnessite peaks.[3,5,7] Therefore, $MnCl_2$ solution was added slowly in a dropwise manner. The effect of the counteranion was investigated by using $CuSO_4 \cdot 5H_2O$ and $Cu(NO_3)_2$.[3,5,7] On the basis of XRD data, the incorporation of the cation seems to be more effective with $CuSO_4$ as indicated by the almost complete disappearance of the peaks associated with the layered phase. In the synthesis of [Cu]−OMS-1, hydrothermal conditions were explored.[1−3,5,7]

In the synthesis of Cu−OMS-2, the sol−gel method was not very advantageous compared to the reflux method in incorporating Cu^{2+} ions.[23] Paramelaconite, a copper oxide, is readily formed in the sol−gel method based on XRD analysis of the product. The amount of Cu incorporated in OMS-2 by the reflux method is very minute. Table 1 gives the labels of the OMS samples that will be used in this paper and their corresponding amounts of Cu in weight percent determined by ICP-AES analysis.

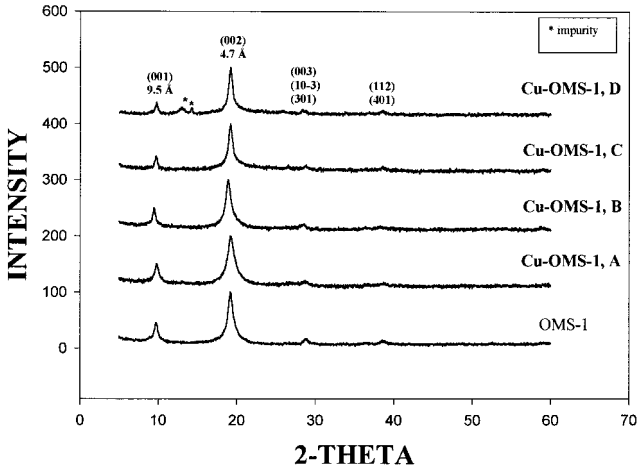

Figure 1. XRD patterns for OMS-1 and Cu−OMS-1 series.

Table 1. Weight % of Cu in the Cu-Containing OMS Materials by ICP Analysis

sample	% Cu	sample	% Cu
Cu−OMS-1, A	1.660	(Cu)−OMS-1, A1	0.8850
Cu−OMS-1, B	3.000	(Cu)−OMS-1, B1	0.8551
Cu−OMS-1, C	13.67	(Cu)−OMS-1, C1	0.9112
Cu−OMS-1, D	23.25	(Cu)−OMS-1, D1	1.146
OMS-2	0		
Cu−OMS-2, A2	0.0171		
Cu−OMS-2, B2	0.0245		
Cu−OMS-2, C2	0.0334		

The XRD patterns of the Cu−OMS-1 materials containing various amounts of Cu incorporated before hydrothermal treatment are shown in Figure 1. The diagnostic peaks for todorokite are present at about 9.5 (001) and 4.7 Å (002).[1,2] The XRD patterns of Cu−OMS-1 materials compared to OMS-1 show much broader peaks which suggest that the former are characterized by smaller particles and larger surface areas (up to 250 m^2/g) than the latter (<50 m^2/g). The XRD pattern of the Cu−OMS-1 material labeled D with 23.2% by weight Cu shows an impurity with additional peaks appearing at 6.2 and 6.8 Å, which may be due to birnessite-related phases such as potassium manganese oxide. The XRD patterns of the OMS-1 ion-exchanged with Cu after hydrothermal treatment, labeled as [Cu]−OMS-1 samples, show the diagnostic peaks for todorokite and indicate that they are relatively pure.[1,2] The peaks for this set of materials have the same shape and relative intensity as that of OMS-1. Figure 2 shows the XRD patterns for the OMS-1 materials ion-exchanged with various amounts of copper(II) ions.

The XRD patterns for the Cu−OMS-2 series prepared by the reflux method showed a peak at 1.9 Å due to paramelaconite, a copper oxide. The peak corresponding to this phase increases as the concentration of copper increases in the refluxed solution.

B. Manganese Oxidation State and Elemental Analysis. Figure 3 summarizes the manganese oxidation states of the different materials as a function of the amount of Cu incorporated in their structures. The average oxidation state of Mn in OMS-1 is 3.50 ± 0.01 which is in very good agreement with previous measurements.[5] The average oxidation state of Mn for the series of Cu−OMS-1 materials increases with the

(17) Vileno, E.; Ma, Y.; Zhou, H.; Suib, S. L *Micropor. Mesopor. Mater.* **1998**, *20*, 3−15.
(18) Guillaume, B.; Xinhua, C.; Chui, W. L.; Kevan, L. *J. Am. Chem. Soc.* **1992**, *114*, 3720−3726.
(19) Vedrine, J. C. *Catalyst Characterization: Physical Techniques for Solid Materials*; Imelik, B., Vedrine, J., Eds.; Plenum Press: New York, 1994.
(20) Veprek, S.; Corke, D. L.; Kehl, S.; Oswald, H. R. *J. Catal.* **1986**, *100*, 250−263.
(21) D'Huysser, A.; Lerebours-Hannover, B.; Lenglet, M.; Bonnelle, J. P. *J. Solid State Chem.* **1981**, *39*, 246.
(22) Kanungo, S. B. *India J. Chem.* **1987**, *26*, 373−383.
(23) Shirley, D. A. *Phys. Sci.* **1975**, *11*, 17.

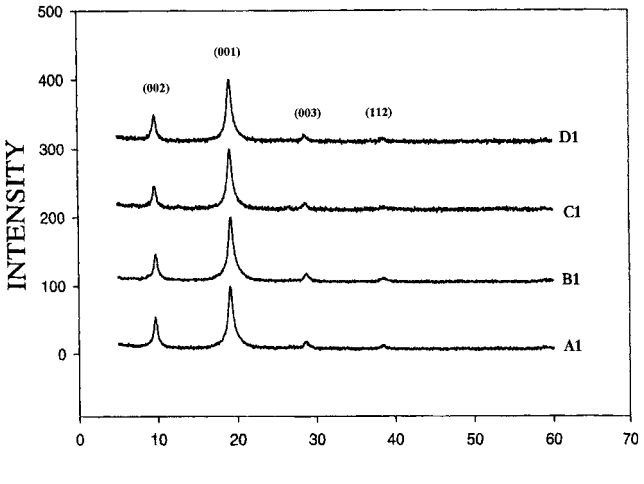

Figure 2. XRD patterns for [Cu]−OMS-1 series.

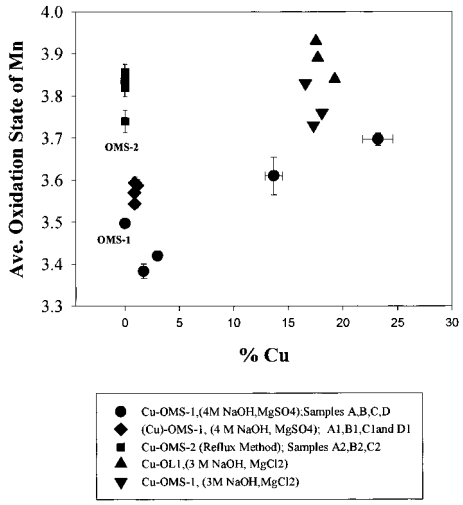

Figure 3. Average oxidation state of manganese as a function of copper content.

amount of Cu incorporated in the structure. The Mn average valency for the materials prepared at pH 3.0 and using $MgCl_2$ was higher compared to the materials prepared at pH 4.0 and using $MgSO_4$. The Cu−OL-1 materials also showed higher oxidation states than their Cu−OMS-1 counterparts. The Cu−OMS-1 materials were prepared from Cu−OL-1. The possible interference of Cu^{2+} ions in reaching the endpoint in the titration of Mn^{2+} was checked by analyzing a blank with Cu^{2+} ions in solution. The amount of titrant used to reach the endpoint was the same for the blank and the one spiked with copper(II) ions. For the series of [Cu]−OMS-1 materials, the average oxidation states of Mn do not change much with the minimal amount of Cu incorporated in their structures. The manganese valency for OMS-2 and the Cu−OMS-2 materials prepared by the reflux method is always about 3.8.[5]

Elemental analyses for Cu−OMS-1 show that the amounts of Mn and Mg decrease sharply as the amount of Cu increases. A plot of the Mg/Mn molar ratio for the two sets of materials is shown in Figure 4. The Mg/Mn molar ratio for the [Cu]−OMS-1 series approaches that of OMS-1. At low concentration of copper, the amount of magnesium decreases slightly. As the amount of copper incorporated in the structure increases, the Mg/Mn molar ratio drops drastically. These data suggest

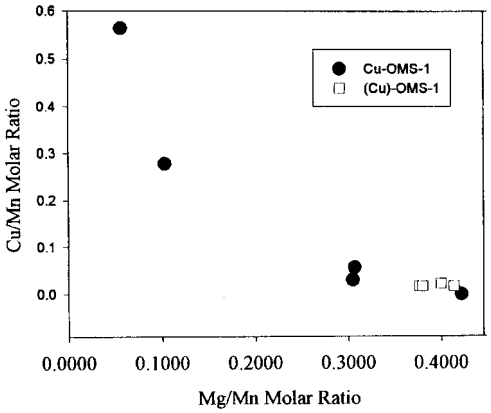

Figure 4. Cu/Mn molar ratio versus Mg/Mn molar ratio.

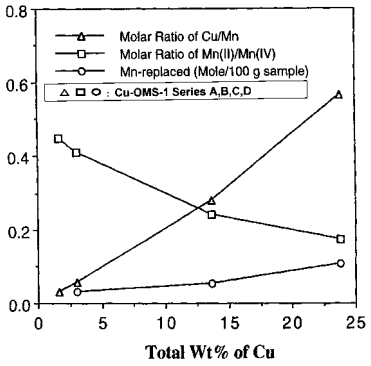

Figure 5. Effect of doping in the Cu−OMS-1 series.

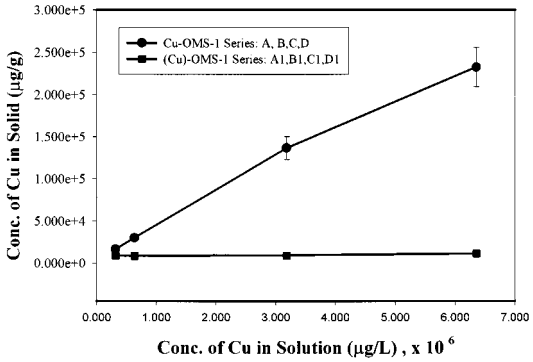

Figure 6. Ion-exchange isotherm for the OMS-1 structure in Cu(II) solutions with overnight stirring at 60 °C.

that small amounts of Mg^{2+} and considerable manganese ions are exchangeable. Figure 5 shows the effect of doping in Cu−OMS-1 samples. The molar ratio of Mn^{II}/Mn^{IV} decreases as % by weight Cu increases. The amount of Mn replaced in mole per 100 g of sample reaches 0.05 for C which has about 13% Cu.

An ion-exchange isotherm for OMS-1 with Cu^{2+} ions is given by Figure 6. This shows that more Cu can be incorporated into the OMS-1 structure when the Cu^{2+} was ion-exchanged before hydrothermal treatment. The OMS-1 tunnels that contain Mg^{2+} can accommodate only minute amounts of the exchanging copper cations. The Mg^{2+} ions that occupied the tunnels were difficult to replace.

C. Thermal Analyses. TGA profiles of OMS-1 and Cu−OMS-1 samples in nitrogen and oxygen streams show a first weight loss for all curves which occurs at 30−150 °C.[2,13] This may be due to water physically sorbed on the surface. The first weight loss for all

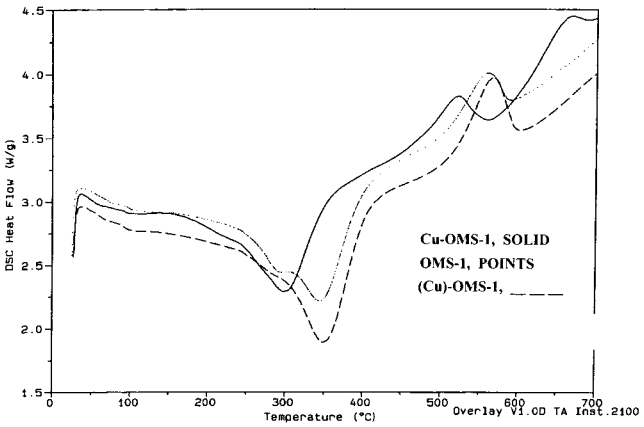

Figure 7. DSC profiles in N_2 from room temperature to 900 °C at 10° C/min.

Table 2. Thermal Stability of Cu-Containing OMS Materials

sample	in nitrogen, °C	in oxygen, °C	sample	in nitrogen, °C	in oxygen, °C
A	397.61	595.20	**A1**	461.00	600.00
B	393.90	570.42	**B1**	451.64	592.49
C	361.90	500.00	**C1**	465.73	590.61
D	356.82	432.86	**D1**	479.10	585.00
OMS-2	630.00	818.09	**A2**	533.00	800.00
OMS-1	430.00	620.00	**B2**	533.00	800.00
			C2	600.00	700.00

samples ranges from 0.86 to 1.50% except for C that has a weight loss of 1.91% in a nitrogen stream and 1.58% in an oxygen stream. The second weight loss below 400 °C in the TGA profile is usually attributed to the dehydration of crystal water in the structure. Weight loss at temperatures above 400 °C may be attributed to oxygen evolution. The amount of stability achieved in the oxygen stream based on the difference in the nitrogen and oxygen curves between 400 °C and the onset temperature for the phase transition around 500 °C are calculated as follows: 1.39% for OMS-1, 0.93% for A, 0.63% for B, and 0.59% for C, and 0.26% for D. Samples C and D show an additional weight loss around 600 °C in nitrogen. Table 2 summarizes the thermal stability of the Cu−OMS-1, [Cu]−OMS-1, and Cu−OMS-2 series.

DSC profiles in N_2 for OMS-1, C, and D1 are shown in Figure 7. OMS-1 loses its tunnel water gradually as represented by the two endotherms in the DSC profile. Material C exhibits an endotherm centered at 351 °C and an exotherm centered at 565 °C. Cu−OMS-1 labeled C loses its tunnel water in one step and at a much lower temperature compared to OMS-1. Loss of tunnel water is believed to occur at temperatures lower than loss of framework- bound hydroxyl groups.[4,6,13] D1 exhibits an endotherm and an exotherm both around 351 °C. Structure collapse in these materials is associated with an exotherm on the basis of XRD and BET data.[1,2] XRD patterns of the materials run after thermal treatment indicate the formation of hausmannite both in N_2 and O_2 for Cu−OMS-1; for Cu−OMS-2, bixbyite is the final product of heating to 900 °C both in N_2 and O_2. Hausmannite (Mn_3O_4) is a spinel type of manganese oxide with Mn^{2+} and Mn^{3+} in a tetragonal structure. Bixbyite (Mn_2O_3) has an anion-deficient fluorite structure.

D. Scanning Electron Microscopy. In the Cu−OMS-1 series, B, which has smaller amounts of Cu incorporated in its structure, has more plates as compared to C. SEM photographs revealed more fibers for material C than B. The fibers have dimensions of about 100−130 nm in width and 2−6 μm in length. Similar results were earlier observed.[3,5,7]

E. Resistivity Measurements. The resistivity of Cu−OMS-1 decreases and levels off as the concentration of Cu increases. The resistivities of this series of materials are in the range of 10^5 to 10^6 Ω cm at 298 K. In contrast, resistivity values for Cu−OMS-2 are on the order of 10^2 Ω cm at 298 K and increase with the amount of Cu incorporated in the structure. There was no observable change in the resistivity of the [Cu]−OMS-1 series.

F. EPR Measurements. EPR spectra for Cu−OMS-1 C showed two sets of six hyperfine signals of Mn^{2+} at 110 K with g values of 2.07 and 2.03 as reported earlier.[3] Hyperfine splittings of 97 and 99 G indicate that Mn^{2+} cations are present in an octahedral environment.[9] The two sets of Mn^{2+} signals may be attributed to different crystallographic sites in the copper-containing OMS-1 structures. Pure OMS-1 sample gave one very broad band. The single intense broad line may be attributed to high manganese(II) content in the OMS-1 structure. After copper incorporation, the amount of Mn(II) decreases and the hyperfine structures were observed. Previous EPR studies on Mn(II) assign the lines observed between the six main hyperfine lines to $\Delta m = \pm 1$ forbidden transitions.[18]

The four hyperfine signals due to Cu^{2+} are observed to have a splitting of 92 G. The g value for the perpendicular component of the Cu^{2+} signals is 2.07. The g value is an important parameter in EPR, which provides considerable information about the electronic structure of the paramagnetic substance relative to the g value of 2.0023 for a free electron. For transition metal ions, deviations of the g value from that of the free electron may arise from spin−orbit coupling effects. No EPR signal was observed for these Cu−OMS-2 materials perhaps due to the low [Cu^{2+}] or due to quenching. This is in contrast to the weak EPR signals previously observed for Cu−OMS-2.[3]

G. X-ray Photoelectron Spectroscopy. XPS was carried out essentially to determine the oxidation states of Cu and possibly to locate the cations in the structure. For transition metal oxides, charge transfer from the ligand toward the metal, which corresponds to np(ligand) → 3d (metal) type transitions, accounts for the appearance of shake-up peaks.[19,20] Paramagnetic transition metal ions such as Ni^{2+} and Cu^{2+} have been observed to exhibit shake-up lines. Cu^{2+} has been established to have satellite features while Cu^{+} does not.[19,20] Hence, this technique was utilized to determine the state of Cu in the different OMS preparations. XPS spectra in the Cu 2p region show spin−orbit split $2p_{1/2}$ and $2p_{3/2}$ peaks along with shake-up satellites for Cu in the 2^+ state for representative samples of the Cu−OMS-1, [Cu]−OMS-1, and Cu−OMS-2. Table 3 summarizes the binding energy values in the Cu 2p region.

The main peak for the Cu $2p_{3/2}$ transition for all samples occurs near 934.5 eV which indicates Cu^{2+} in an octahedral environment.[21] Figure 8 shows a detailed

Table 3. Binding Energies (eV) of Cu 2p Signals from Cu−OMS Materials[a]

	Cun-OMS-1 A	Cu−OMS-1 D	(Cu)−OMS-1 D1	Cu−*OMS-2* B2
Cu $2p_{3/2}$	942.68	943.68	943.39	942.13
Cu $2p_{3/2}$	941.65	941.89	941.71	*933.09*
Cu $2p_{3/2}$	*933.47*	*934.23*	*932.93*	
Cu $2p_{1/2}$	962.04	962.22	962.24	962.05
Cu $2p_{1/2}$	*953.25*	*954.12*	*952.85*	*952.86*

[a] Italicized values correspond to the main peak transitions.

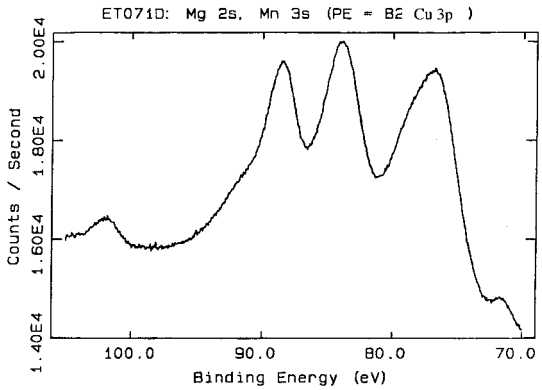

Figure 8. Detailed XPS spectrum for the Cu 3p transition for Cu−OMS-1 C.

XPS spectrum showing a Cu 3p transition from Cu−OMS-1 C. The binding energies (B.E.'s) for the Mn $2p_{3/2}$ and Mn $2p_{1/2}$ transitions from OMS-1, A, C, and D1 are centered at 642.2 and 653.9 eV, respectively. These binding energies suggest that Mn in the sample is mainly in the 4^+ oxidation state.[22] Spectra of the Mn 2p region of Cu−OMS-2 labeled B2 show a peak for the Mn $2p_{3/2}$ transition with a B.E. centered at 641.97 eV, suggesting that the Mn is close to the Mn^{3+} state.[23] The Mn 3s multiplet splitting indicates the presence of multivalent Mn. XPS spectra for Cu−OMS-2 in the Mn 3s region show multiplet splitting with B.E.'s of 88.71 and 84.09 eV. This is consistent with reports that the OMS-2 structure contains Mn^{3+} and Mn^{4+}.[24]

H. Catalytic Evaluation for the Oxidative Dehydrogenation of Ethylbenzene to Styrene. Plots of percentage conversion as a function of reaction time for copper containing OMS-1 structures show an initial activity after which the percent conversion drops and becomes steady for up to 12−15 h of reaction time. OMS-1 has the lowest conversion and selectivity at around 22% and 8%, respectively, while Cu−OMS-1 C gave the highest conversion and selectivity around 50% and 16%, respectively. The [Cu]−OMS-1 labeled D1 showed comparable performance as that of Cu−OMS-1, C. The conversions over OMS-2 and A2 decrease with time. A plot of % selectivity to styrene as a function of Cu content in the structure after 6 h of reaction time is given in Figure 9. These preliminary data suggest that copper content does influence styrene selectivity. Detailed studies of selectivity at constant conversion and characterization of catalysts during and after reaction need to be carried out to provide enhanced understanding of these preliminary data.

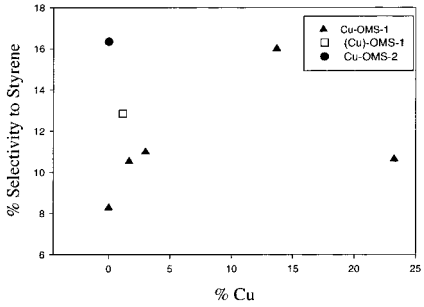

Figure 9. Percentage selectivity to styrene versus % by weight copper.

Discussion

Synthesis and Powder X-ray Diffraction. Several types of OMS-1, OMS-2, and OL-1 have been prepared by various synthetic procedures. The different preparations provided different materials that have unique chemical and physical properties. A recent review on octahedral molecular sieves presented a number of these materials with some of their properties such as particle size, color, morphology, crystallinity, average manganese oxidation state, thermal stability, ion-exchange capacity, ion-exchange properties, electrical conductivity, magnetic susceptibility, defect density, and catalytic activity being tailored during synthesis.[24] The series of materials prepared in this study show distinctive features. Relative trends in their chemical and physical properties are established as a function of cation incorporated into its structure, specifically Cu^{2+} ions.

In the Cu−OMS series of materials, ICP-AES analysis shows that the Cu/Mn molar ratio of 0.278 for C is the substitution limit for a pure sample based on its XRD pattern. Earlier studies on terrestrial todorokites show that the Mn^{2+}/Mn^{4+} molar ratio ranges from 0.15 to 0.26.[25−27] This molar ratio was suggested to be the upper limit in molar ratios of trace metal to Mn in marine 10-Å manganates (buserite layer structure) since divalent cations such as Ni^{2+} and Cu^{2+} can readily substitute for Mn^{2+}.[28] However, other studies using synthetic 10-Å manganates reveal that the molar ratios of incorporated metals to Mn vary with the nature and concentration of the cations in the substituting suspension.[29] In other words, different syntheses lead to varying degrees of cation uptake capacity. Hence, results of cation uptake studies must be reported with caution. However, this could prove to be an advantage in designing the desired cation capacity of the material. In the [Cu]−OMS-1 series, the amount of copper(II) ions that can exchange into the tunnel is very small. The Mg^{2+} ions are relatively stable in the tunnels of OMS-1 balancing the charge developed by incomplete oxidation or replacement of Mn^{4+} ions by Mn^{2+}, Mg^{2+}, or Mn^{3+} in the framework. The cation uptake of Cu−OMS-2 prepared by the reflux method is also very low. This may be due to preference of the [2 × 2] structure for a monovalent cation to balance the charge on the structure, which

(24) Suib, S. L. In *Recent Advances and New Horizons in Zeolite Science and Technology Studies*; Chua, S. I. W., Park, S. E., Eds.; Surface Science and Catalysis; Elsevier Science B. V.: New York, 1996; Vol. 102, pp 47−74.

(25) Frondel, C.; Marvin, U. B.; Ito, J. J. *Am. Mineral* **1960**, *45*, 1167−1173.

(26) Levinson, A. A. *Am. Mineral.* **1960**, *45*, 802−807.

(27) Straczek, J. A.; Horen, A.; Ross, M.; Warshaw, C. *Am. Mineral.* **1960**, *45*, 1174−1184.

(28) Buen, V. M.; Buen, R. G. *Sci. Lett.* **1978, *39***, 341−348.

(29) Lei, G. *Mar. Geol.* **1996**, *133*, 103−112.

contains Mn^{3+}. Natural materials having the 2 × 2 structure can contain divalent cations.

Cu^{2+}-Substitution in Framework and Tunnel Sites. The success of preparing synthetic counterparts of the minerals and manganates in manganese nodules continually contribute to the ever growing applications of these materials in catalysis, electrochemistry and battery applications, and adsorption chemistry. However, the exact mechanism by which layered materials form tunnels of varying sizes and how a number of species are accommodated into the structures still merits systematic and detailed investigation.

This study provides several indications that Cu^{2+} may be incorporated not only in the tunnels of OMS-1 but also substitute for either Mg^{2+} originally doped in the framework for structure stability or replace some $Mn^{3+,2+}$ in the OMS-1 framework under hydrothermal conditions.

The XPS data of Table 3 and corresponding spectra show that there are different species in each of these samples. Sample [Cu]-OMS-1 (D1) has low Cu $2p_{3/2}$ and Cu $2p_{1/2}$ signals in relation to all other Cu−OMS-1 materials. We believe that this lowering of binding energy is indicative of Cu^{2+} in the framework which is in a more reduced (lower binding energy) state. This would be indicative of a covalent interaction. The higher binding energies for the nonframework materials Cu−OMS-1 A and D are more indicative of ionic states and are attributed to locations of cations in tunnel sites. A comparison of the three copper−OMS-1 systems shows a lowering of the most intense Cu $2p_{3/2}$ transition ranging from 0.54 to 1.3 eV, which are readily measured and clearly different. Note that the lowest energy Cu $2p_{1/2}$ transition for [Cu]−OMS-1 is also lowered by 0.4 to 1.3 eV, exactly the same trend as the Cu $2p_{3/2}$ transition. These data suggest that the most reduced Cu transitions are framework species in sample [Cu]−OMS-1, sample D1.

The other Cu $2p_{3/2}$ and Cu $2p_{1/2}$ transitions of high binding energy are due to tunnel cation species bound as oxidic and hydroxyl species. These data clearly show that the framework substituted sample D1 also contains some tunnel Cu^{2+} cations, which is not unexpected. Further support for framework substitution comes from X-ray excited Auger transitions which clearly show two peaks for the framework substituted [Cu]−OMS-1 and only one broad peak for the tunnel substituted systems. It is difficult to obtain quantitative data for the various copper species without deconvolution. The XPS region for manganese is quite complicated due to the mixed valency of these systems which leads to a broadening of these transitions and again deconvolution is needed to distinguish Mn^{2+}, Mn^{3+}, and Mn^{4+}. Nevertheless, these data are entirely consistent with data from EPR experiments.

The XPS data of Figure 8 clearly show two different peaks at 84.09 and 88.71 eV which are believed to be due to Mn 3s transitions for mixed-valent manganese species. The Cu 3p transitions ($^1/_2$ and $^3/_2$) near 75 eV are clearly broad and unresolved. The broad peak above 90 eV is believed to be due to small amounts of Mg (Mg 2s). The XPS data suggest that when Cu^{2+} is introduced before autoclave treatment of Cu−OL-1 or [Cu]−OL-1 that only this copper can be incorporated into the framework as evidenced by substantial lowering of the Cu $2p_{1/2}$ and Cu $2p_{3/2}$ transitions.

Table 4. Effective Ionic Radii of Template Cations

cation	coordination number	effective ionic radius, Å[a]
Mg^{2+}	6	0.72
Cu^{2+}	6	0.73
Mn^{2+}	6	0.67
Mn^{3+}	6	0.65
Mn^{4+}	6	0.53

[a] Shannon, R. D. *Acta Crystallogr.* **1976**, *A32*, 7510.

In the synthesis of Cu−OMS-1, the Cu^{2+} ions can easily substitute for the divalent cations (Mg^{2+}, Mn^{2+}) either in the tunnel or framework on the basis of similarity in ionic radii. Table 4 gives a summary of these ionic radii. The presence of Cu^{2+} ions decreases the Mn^{2+}/Mn^{4+} ratio in Cu−OMS-1 samples as suggested by an increasing trend in the average oxidation state of Mn and decreasing amount of total Mn from elemental analysis and Mn average oxidation state determination.

The decreasing amount of Mg^{2+} as concentration of Cu^{2+} increases in Cu−OMS-1 indicates that some Mg^2 ions are also being replaced by Cu^{2+}. At low concentration of the substituting cation in solution, it is possible that Cu^{2+} ions simply displace some of the Mg^{2+} ions in the Mg−OL-1 interlayer sites. During hydrothermal synthesis, Cu−OL-1 possessing a large amount of Cu^{2+} in the layer sheets may compete for framework sites and replace the $Mn^{3+,2+}$and Mg^{2+} during reactions that possibly occur under hydrothermal conditions. From elemental analysis, the amount of Mg in Cu−OMS-1 C is less than 2 wt %. In the synthesis of OMS-1 from OL-1, Mg^{2+} doping was found to be a key factor in the transformation and production of a thermally stable todorokite-type structure.[2,30]

On the basis of charge balance supported by analytical analysis, about 3 wt % Mg^{2+} can occupy framework sites in OL-1 which stabilizes the layers and transforms into the tunnel OMS structure.[1−2,30] With relatively abundant hydrated Cu^{2+} ions incorporated in the layered structure, framework substitution may occur under conditions of hydrothermal synthesis. Framework substitution of Mg by Cu explains the trends in the thermal analyses of the materials prepared. The [Cu]−OMS-1 series exhibit similar stability as OMS-1 since Cu^{2+} ions reside only in the tunnel.

The amounts of Mg in these materials are almost constant. Cu−OMS-1 A and B actually have Mg/Mn molar ratio close to that of the [Cu]−OMS-1 series with Cu^{2+} ions in the tunnel. The absence of Mg framework substitution at low Cu^{2+} concentration probably accounts for the relative stability of A and B over C and D. The presence of Mg^{2+} in the OL-1 framework stabilizes the octahedral chain and readily converts the layered phase into a thermally stable OMS-1.[24]

Framework substitution of Mg^{2+} and $Mn^{3+,2+}$ by Cu^{2+} in C and D also explains the trends in Mn oxidation state and resistivity. The Mn average valency increases with the amount of Cu possibly due to substitution of Mn^{2+} and even Mn^{3+}. The replacement of $Mn^{3+,2+}$ ions

(30) Tian, Z. R.; Yin, Y. G.; Suib, S. L. *Chem. Mater.* **1997**, *9*, 1126−1133.

by M^{2+} ions in the framework necessitates the presence of cations to counterbalance the charge that develops in the structure unless defects such as oxygen vacancies occur.[30] With Cu^{2+} in the framework replacing $Mn^{3+,2+}$, Mn will primarily be 4+, hence, its average oxidation state will increase. This substitution in the framework possibly led to more defects in the structure, which may account for the observed thermal instability.[30−32]

The amount of stability achieved by samples C and D in an oxygen stream before tunnel collapses was smaller than OMS-1 and Cu−OMS-1 with low Cu content. This might be attributed to a decrease in the amount of $Mn^{3+,2+}$ in the framework. A single [3 × 3] tunnel in the todorokite structure shows that the central M1 and M3 octahedra are occupied only by Mn^{4+} and that of M2 and M4 sites by lower valency cations such as Mn^{3+}, Mg^{2+}, Ni^{2+}, Cu^{2+}, etc.). The Cu^{2+} may substitute for Mn^{2+} and Mg^{2+} in the M2 site which is significantly distorted from octahedral symmetry. Jahn−Teller stabilized Cu^{2+} may also be favorably accommodated in the M4 site which is the most distorted octahedron.[11,30] There is no evidence of extraframework copper oxides on the surface of these materials.

In the resistivity measurements, the trend for Cu−OMS-1 is consistent with doping. Electrical conductivity which is proportional to the inverse of resistivity is governed by framework doping.[32] Framework substitution by Cu^{2+} which leads to lower level of mixed Mn valency possibly accounts for the decrease in resistivity as Cu concentration increases. The low resisitivity of OMS-2 materials had been attributed to its low level of mixed valency, having an average Mn oxidation state of 3.8.[7] Sites of low valency had been suggested to act as traps which makes it difficult for electron hopping to occur perhaps due to the need for multi-electron-transfer events which may be due to less overlap due to the smaller radial distribution of Cu^{2+} orbitals.

XPS data reveal that Cu remains in the 2+ state as indicated by the shake-up peaks associated with Cu in such valency. However, XPS spectra of Cu−OMS-1 C showed a peak in the Cu 3p region, which was not observed for Cu−OMS-1 B and [Cu]-OMS-1 D1. The additional peak could be due to different Cu^{2+} in C, i.e., in the framework. Additional peaks in XPS may be attributed to configuration interactions that are due to different transitions.[19,20] The EPR spectra of Cu−OMS-1 and [Cu]−OMS-1 suggest a lack of electronic delocalization in their structures. The two sets of Mn^{2+} signals may be due to a difference in their crystallographic sites or presence of additional EPR transitions caused by Jahn−Teller transitions upon copper incorporation.

A scheme for a possible mechanism for the synthesis of Cu−OMS-1 under hydrothermal conditions is shown in Figure 10a.[1,2,9] A detailed mechanism for the possible substitution of Cu^{2+} in the framework under hydrothermal conditions is presented in Figure 10b.[3,5,7]

Olation and oxolation are two mechanisms by which hydrolyzed metal ions undergo condensation.[33] Olation involves nucleophilic attack on a positively charged

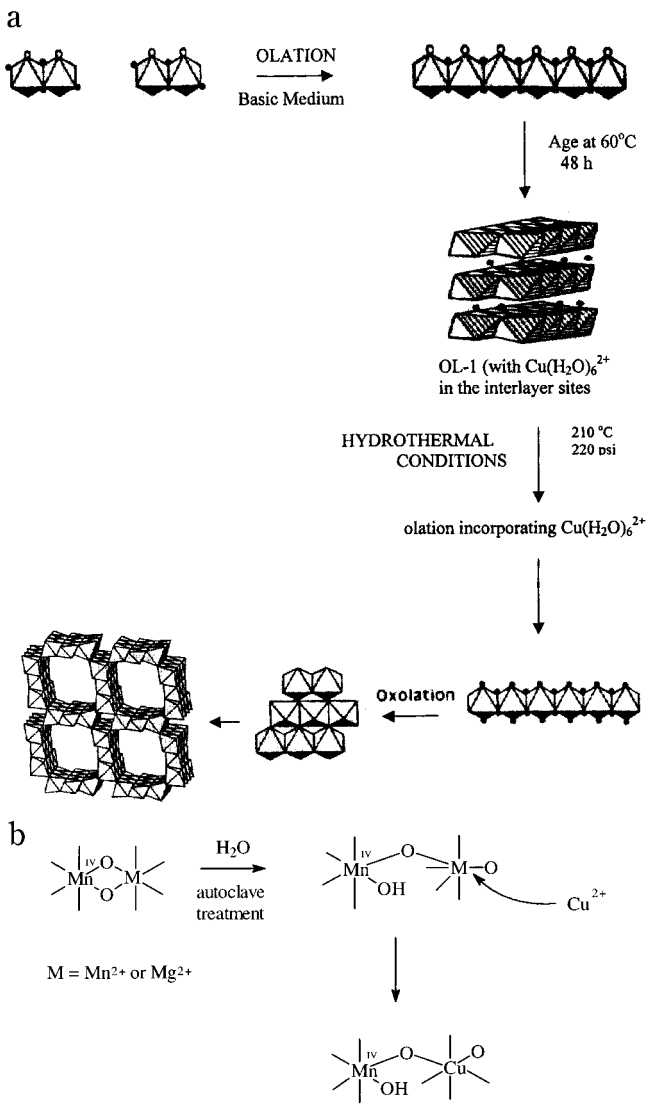

Figure 10. (a) Scheme for possible mechanism of Cu^{2+} incorporation during conversion of OL-1 to tunnel material under hydrothermal conditions and (b) detailed schematic of possible mechanism of copper incorporation in the framework under hydrothermal conditions.

cation by a negatively charged OH group which results in the departure of an aquo ligand from the coordination sphere of the metal. The process, which involves the formation of "ol" bridges (eq 1), is possible only with aquo precursors having their maximum coordination number.

$$M{-}OH + M{-}OH_2 \rightarrow OH^- M + H_2O \qquad (1)$$

Oxolation involves two hydroxo groups reacting to form an "oxo" bridge accompanied by release of a water molecule. The reaction (eq 2) occurs via nucleophilic addition of OH groups on the metal ions followed by a 1,3 proton transfer in the transition state so that water molecules can be easily removed.

$$M{-}OH + HO{-}M \rightarrow M{-}O{-}M + H_2O \qquad (2)$$

In the preparation of Cu−OMS-1 systems, layered birnessite was ion-exchanged with Cu^{2+} before hydrothermal synthesis to form synthetic buserite. Cu-$(H_2O)_6^{2+}$ ions occupy the interlayer sites and stabilize

(31) Burns, R. *Mineralogical Applications of Crystal Field Theory*, 2nd ed.; Cambridge University Press: Cambridge, 1993; pp 338−348.
(32) Tian, Z. R.; Yin, Y. G.; Suib, S. L.; O'Young, C. L. *Chem. Mater.* **1997**, *9*, 126−1133.
(33) Henry, M.; Jolivet, J. P.; Jacques, L. *Struct. Bonding* **1992**, 180−186.

the layer structure forming Cu−OL-1. Under hydrothermal conditions deoxolation may occur followed by an olation wherein $Cu(H_2O)_6^{2+}$ may now form an "ol" bridge with framework Mn. An internal proton transfer may occur followed by oxolation to give corner-sharing octahedral chains. Cu−OMS-1 with high Cu/Mn ratio exhibit unique properties different from OMS-1 and OMS-1 with low Cu content. The differences in their properties may be attributed to framework substitution of Mn^{2+} and Mg^{2+} at high Cu content in the layers of OL-1 that occurred under hydrothermal conditions.

Reactivity as a Function of Copper Content. The reaction carried out in the absence of OMS materials did not progress. The OMS materials provide lattice oxygens needed for partial oxidation. The other product observed from GC-MS was CO. The rates of conversion seem to correlate with increasing Cu content of the material. This may be due to the presence of more defect sites in these materials. The exact mechanism by which the reaction occurs in the presence of the catalyst is still under study.

Previous studies on the mechanism of activity of Hopcalite ($CuMn_2O_4$) which is an important catalyst in respiratory protection in military, mining, and space applications, reported that the formation of cation vacancies in the bulk and formation of CuO at the surface may be the driving force for its observed catalytic performance.[34,35] This might be the case for the OMS materials which begins to lose its tunnel structure early on in the reaction and form a spinel-type Mn_3O_4 material based on XRD analyses of the consumed material. The presence of CuO at the surface of the material still has to be confirmed. Further investigation has to be done to characterize the material after reaction. XPS will be a useful technique in monitoring and characterizing the catalyst. Studies are also being done to test the activity of commercially available Mn_3O_4. If the spinel formed from OMS materials is more active than the commercially available manganese oxide, then optimization of reaction conditions using Cu−OMS-1 C should be carried out.

(34) Kanungo, S. B. *J. Catal.* **1979**, *58*, 419.
(35) Puckhaber, L.S.; Cheung, H.; Cocke, D. L.; Clearfield, A. *Solid State Ionics* **1989,** *32/33,* 206.

Conclusions

These studies focused on manganese octahedral molecular sieves and clearly show that their compositional, electronic, electrochemical, conductivity, adsorptive, and catalytic properties are very promising and can be tailored to meet specific applications. More Cu can be incorporated into the OMS-1 structure when Cu^{2+} ions was ion-exchanged before hydrothermal synthesis than after hydrothermal treatment. Elemental analyses, manganese oxidation state determinations, XPS, TGA, and DSC results provide the basis for framework substitution under hydrothermal conditions. The average oxidation state of Mn in the Cu−OMS-1 series increases with increasing amount of Cu incorporated either in tunnel or framework sites. The average oxidation of Mn in the [Cu]−OMS-1 series does not change with the small amount of Cu in the tunnel. The same is true for the CuOMS-2 series. The Cu(II) ions easily substitute for the divalent cations (Mg^{2+}, Mn^{2+}) in OL-1 and OMS-1. The thermal stabilities of OMS-1 and OMS-2 structures decrease as the amount of Cu incorporated increases. The Cu incorporated in the structures, especially those in the framework, can be considered as defects in the structure which leads to less thermally stable but more catalytically active systems. Resistivity decreases and levels off as Cu content increases in OMS-1 and increases in the OMS-2 structure. The electrical conductivity properties of the Cu−OMS materials are typical of semiconductors.

On the basis of the survey of catalytic activity of OMS structures containing various amounts of Cu for the oxidative dehydrogenation of ethylbenzene to styrene at such a relatively low temperature of 300 °C, Cu−OMS-1 C which has more defects in its structure possibly due to framework substitution gave the best catalytic results with 16% selectivity and 50% conversion.

Acknowledgment. E.N.-T. and S.L.S. thank the Engineering and Science Education Project, Department of Science and Technology, Philippines, for support. We thank the U.S. Department of Energy, Office of Basic Energy Sciences, Division of Chemical Sciences for support of this research.

CM9811040